LBL-16842 c.2
Preprint

Lawrence Berkeley Laboratory

UNIVERSITY OF CALIFORNIA

Materials & Molecular Research Division

RECEIVED
LAWRENCE
BERKELEY LABORATORY
APR 17 1984
LIBRARY AND
DOCUMENTS SECTION

Submitted to Acta Metallurgica

FATIGUE CRACK PROPAGATION IN OIL ENVIRONMENTS: PART II: A MODEL FOR CRACK CLOSURE INDUCED BY VISCOUS FLUIDS

J.-L. Tzou, C.H. Hsueh, A.G. Evans, and
R.O. Ritchie

December 1983

TWO-WEEK LOAN COPY

This is a Library Circulating Copy which may be borrowed for two weeks. For a personal retention copy, call Tech. Info. Division, Ext. 6782.

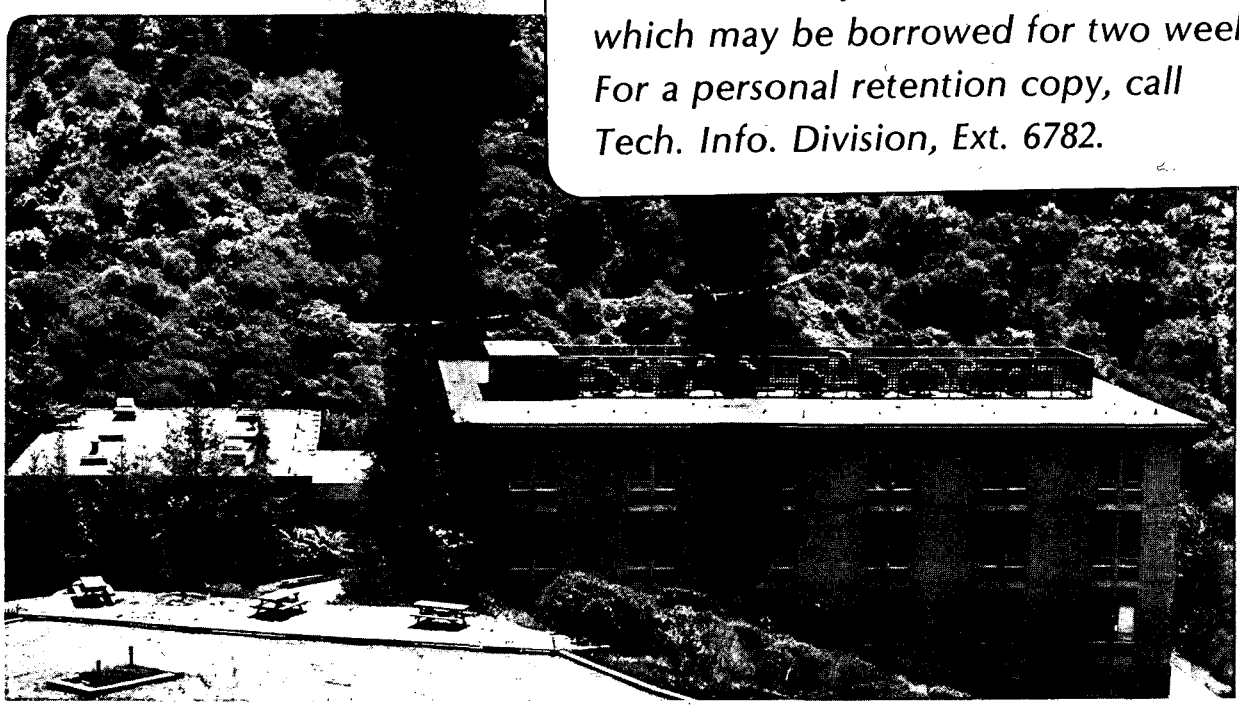

LBL-16842 c.2

Prepared for the U.S. Department of Energy under Contract DE-AC03-76SF00098

DISCLAIMER

This document was prepared as an account of work sponsored by the United States Government. While this document is believed to contain correct information, neither the United States Government nor any agency thereof, nor the Regents of the University of California, nor any of their employees, makes any warranty, express or implied, or assumes any legal responsibility for the accuracy, completeness, or usefulness of any information, apparatus, product, or process disclosed, or represents that its use would not infringe privately owned rights. Reference herein to any specific commercial product, process, or service by its trade name, trademark, manufacturer, or otherwise, does not necessarily constitute or imply its endorsement, recommendation, or favoring by the United States Government or any agency thereof, or the Regents of the University of California. The views and opinions of authors expressed herein do not necessarily state or reflect those of the United States Government or any agency thereof or the Regents of the University of California.

LBL-16842

FATIGUE CRACK PROPAGATION IN OIL ENVIRONMENTS:
PART II: A MODEL FOR CRACK CLOSURE INDUCED BY VISCOUS FLUIDS

J.-L. Tzou, C. H. Hsueh, A. G. Evans and R. O. Ritchie

Materials and Molecular Research Division,

Lawrence Berkeley Laboratury

and

Department of Materials Science and Mineral Engineering,

University of California, Berkeley, CA 94720

December 1983

This work was supported by the Director, Office of Energy Research, Office of Basic Energy Sciences, Materials Science Division of the U.S. Department of Energy under Contract No. DE-AC03-76SF00098.

FATIGUE CRACK PROPAGATION IN OIL ENVIRONMENTS:

PART II: A MODEL FOR CRACK CLOSURE INDUCED BY VISCOUS FLUIDS

J.-L. Tzou, C. H. Hsueh, A. G. Evans and R. O. Ritchie

Materials and Molecular Research Division,

Lawrence Berkeley Laboratory

and

Department of Materials Science and Mineral Engineering,

University of California, Berkeley, CA 94720

Abstract - Several mechanisms have recently been identified for fatigue crack closure. The current work examines the concept of crack closure induced by the hydrodynamic wedging action of a viscous fluid within an advancing crack during cyclic loading. Unlike previous analyses, the model considers both the hydrodynamics of the pressure distribution within the crack and the kinetics of the penetration of the fluid into the crack. In addition, the results are presented in fracture mechanics terminology, and expressed as an effective (near tip) stress intensity range. Analyses involving both "full-" and "partial-penetration" of the viscous fluid inside the crack are utilized to rationalize the influence of viscosity on fatigue crack propagation in dehumidified oil environments, described in Part I of this paper. The roles of stress intensity range, crack size and frequency on the development of such fluid-induced crack closure are also examined.

1. INTRODUCTION

Fatigue crack closure involves a reduction in the apparent driving force for crack advance through contact between the mating fracture surfaces during the loading cycle. Plasticity-induced closure, as first postulated by Elber,[1] was originally considered to arise from the elastic constraint in the wake of the crack tip on material elements previously plastically-stretched at the tip. However, it is now known that closure can result from several other sources including crack surface corrosion debris and irregular crack path morphologies coupled with inelastic Mode II crack tip displacements.[2] In such cases, under small-scale yielding conditions, the stress intensity range actually experienced at the crack tip is reduced from the nominal (global) value, ΔK, given by the difference between the applied maximum and minimum stress intensities in the cycle ($\Delta K = K_{max} - K_{min}$), to some lower effective near tip (local) value, ΔK_{eff}, defined as $K_{max} - K_{cl}$, where K_{cl} is the stress intensity to cause closure of the crack surfaces ($K_{cl} \gtrsim K_{min}$).

In the present study the concept of fatigue crack closure induced by a viscous fluid within the crack is considered. The motivation for this work pertains to studies of fatigue crack propagation in oil environments, as described in Part I of this paper.[3] As summarized in Fig. 1, at low load ratios, crack propagation rates (da/dN) in oil **exceed** those in moist air at near-

threshold levels (below $\sim 10^{-6}$ mm/cycle), **are slower than** in moist air at higher growth rates (above $\sim 10^{-6}$ mm/cycle) and show a general trend toward faster crack growth rates in the higher viscosity oils. The first two observations can be attributed to the environmental shielding effect of the dehumidified and chemically inert oils.[3] However, the role of viscosity in influencing behavior at higher growth rates has been ascribed to **viscous fluid-induced crack closure.**[3] In the present paper, a quantitative model for such closure is developed, based on considerations of hydrodynamics, capillary flow and linear elastic fracture mechanics (LEFM). The model treats the development of closure for cracks both partially or fully penetrated by a viscous medium.

2. PREVIOUS WORK

The notion of a viscous fluid inside a fatigue crack providing a cushion between the closing fracture surfaces has been used to explain **both** decreasing **and** increasing lifetimes with increasing fluid viscosity.[4-11] Way[4] first suggested that fluid pressure inside an extending crack could accelerate crack growth, with the less viscous fluid promoting the larger acceleration due to easier penetration into the crack. Galvin and Naylor[7] similarly reasoned that higher growth rates would result from higher fluid pressures, and that the magnitude of this pressure would be a function of the physical properties of the fluid (including viscosity, viscosity-

pressure coefficient, and compressibility). However, the idea of an internal fluid pressure **increasing** growth rates under **cyclic** loading is questionable since fluid pressure must induce a stress intensity, K^*, that <u>decreases</u> the effective stress intensity range,

$$\Delta K_{eff} = K_{max} - (K_{min} + K^*_{max}) \quad , \tag{1}$$

where K_{max} and K_{min} are the nominal values of the maximum and minimum stress intensities, respectively, and K^*_{max} is the value of K^* evaluated at peak loads.

Endo and co-workers[9,10] estimated the magnitude of the fluid pressure and its influence on the applied stresses for crack propagation in rotating bending tests on steels and bearing metals. However, their hydrodynamic model can only be applied to the case of full penetration of fluid to the crack tip and correspondingly predicts increasing fluid pressure, and hence **decreasing** growth rates, with **increasing** fluid viscosity. Although in accord with the majority of their experimental data,[10] the predictions of this model cannot fully rationalize all other results,[6] including those in the present study[3] where the fastest growth rates are found in the higher viscosity oils.

These apparent inconsistencies arise because the magnitude of the closure (i.e., K^*) depends not only upon the fluid pressure generated within the crack but also upon the extent of fluid penetration,[3,4,10] processes which have opposite dependencies on

fluid viscosity. A new quantitative model for viscous fluid-induced crack closure, which treats both the hydrodynamics of fluid pressure and the kinetics of fluid penetration, is developed in this article. The analysis, which is performed both for arbitrary edge crack and compact tension C(T) geometries, permits estimation of the magnitude of viscous fluid-induced crack closure, and hence values of ΔK_{eff}.

3. MODEL FOR VISCOUS FLUID-INDUCED CRACK CLOSURE

3.1 General Considerations

The analysis of crack closure induced by a viscous fluid inside a growing fatigue crack is based on three principal steps, namely i) a hydrodynamic analysis of the resultant fluid pressure under cyclic loading for both full and partial fluid penetration, ii) a LEFM analysis of the resultant stress intensity, K^*, due to the fluid pressure, and iii) superposition of the variation of $K^*(t)$ during the cycle with the variation of applied stress intensities, $K(t)$, to yield the effective (near-tip) stress intensity, $K_{eff}(t)$.

The analysis is conducted using the extent of penetration of the viscous fluid into the crack, d, as a variable. This penetration is governed by capillary action, such that, by idealizing the fatigue crack as a parallel sided slit, of length $\bar{a}$, width B and average crack opening $\langle h \rangle$, the penetration distance, d, can be readily estimated as:[12]

$$d^2(t) = \left(\frac{\gamma \cos\beta}{3\eta\rho} \right) \int_0^t \langle h \rangle (t) dt \quad , \tag{2}$$

where γ is the surface tension of the oil, β the wetting angle between the fluid and the crack wall, η the kinematic viscosity and ρ the density.

The method of analysis is presented in its entirety for one case: complete fluid penetration into an arbitrary tensile edge crack. In this configuration, a fatigue crack of length, a, in a test piece of thickness, B, width, W, and remaining uncracked ligament, b = (W - a), is subjected to remotely applied sinusoidally varying loads, P, such that the nominal stress intensity factor is given by:[13,14]

$$K = \frac{P}{BW^{\frac{1}{2}}} \cdot f(a/W) \quad , \tag{3}$$

where

$$f(a/W) = 1.12 \sqrt{\frac{\pi a}{W}} \quad .$$

Thereafter the corresponding final solutions are provided for three other cases: partial penetration of fluid in the edge crack configuration, and both partial and full penetration in the compact tension C(T) geometry. In the latter case it is assumed that the fluid pressure is only generated within the fatigue crack and not

within the notch, i.e., over a distance $\bar{a} = (a - a_0)$ rather than a, where a_0 is the length of the notch.

3.2 Geometrical Considerations

Following the analysis of Turnbull,[15] the overall shape of the idealized fatigue crack is taken to be trapezoidal (Fig. 3), with crack mouth opening displacement, CMOD = h_m, and crack tip opening displacement, CTOD = h_δ, such that the average crack opening, $\langle h \rangle$, at time t is given by:

$$\langle h \rangle(t) = 1/2[h_m(t) + h_\delta(t)] \quad . \tag{4}$$

The CTOD can be related to the stress intensity, K_{eff}, using small-scale yielding analysis:[16]

$$h_\delta \approx 0.49\left(\frac{K_{eff}^2}{\sigma_y E}\right) \quad , \tag{5}$$

where σ_y is the tensile yield strength and E is the Young's modulus.

The CMOD can then be determined by considering the opening of the fatigue crack about some rational axis at distance, rb, ahead of the crack tip (Fig. 2), where r is the non-dimensional rotational factor that determines the location of the apparent rotational axis in the specimen ligament, b, along the crack line. The rotational factor r takes values varying typically from ~ 0.195 for elastic deformation to ~ 0.470 for plastic deformation,[17] such that:

$$h_m = \left(\frac{a + rb}{rb}\right) h_\delta \quad . \tag{6}$$

Combining Eqs. (4)-(6), we obtain:

$$\langle h \rangle (t) \approx \frac{K_{eff}^2(t)}{4\sigma_y E} \left[\frac{a + 2rb}{rb}\right] \quad , \tag{7a}$$

such that the rate of change of the crack opening becomes:

$$\langle \dot{h} \rangle = \frac{K_{eff} \dot{K}_{eff}}{2\sigma_y E} \left[\frac{a + 2rb}{rb}\right] \quad . \tag{7b}$$

3.3 Stress Intensity from Fluid Pressure

For the case of fluid flow predominately along the crack length (i.e., crack length small compared to thickness), Endo et al.[9] have derived an expression for the distribution of hydrodynamic fluid pressure p(x) at distance x from the mouth along a closing fatigue crack, when fluid fully penetrates the crack (Fig. 3):

$$p(x) = \frac{6\eta\rho\, a^3 \log[1 - (x/a)]\dot{\theta}}{h_m^3} \quad , \tag{8}$$

where $\dot{\theta}$ is the closing angular velocity of the crack walls, which can be approximated by (Figs. 2 and 3):

$$\dot{\theta} \approx - \frac{\dot{h}_m}{(a + rb)} \approx - \frac{2\langle \dot{h} \rangle}{(a + rb)} \quad , \tag{9a}$$

which, on substitution of Eq. (7b), yields:

$$\dot{\theta} \approx -\left[\frac{a + 2rb}{a + rb}\right] \cdot \frac{K_{eff}\,\dot{K}_{eff}}{\sigma_y\,Erb} \quad . \tag{9b}$$

The corresponding fluid pressure distribution when the viscous fluid only partially penetrates the crack, again assuming no thickness direction flow (Fig. 4), is given by:[18]

$$p(x) = \frac{6\eta\rho\langle\dot{h}\rangle\, x(d - x)}{\langle h\rangle^3} \quad . \tag{10}$$

The hydrodynamic wedging action of the viscous fluid within the crack induces a resultant stress intensity due to this fluid pressure, K^*, which modifies the driving force for crack extension (Eq. (1)), as shown in Fig. 5. The magnitude of K^* consists of two components, namely an increase in the effective K_{min}, K_p, and a smaller decrease in the effective K_{max}, K_q, such that the maximum value of K^*, i.e., $K^*_{max} = K_q + K_p$.

Values of K^* can be determined from the fluid pressure distribution p(x) by computing the resultant force (per unit thickness), F, acting on the crack faces during the fatigue cycle and then utilizing the linear elastic stress intensity solutions[14] for edge crack subjected to concentrated forces. For complete fluid penetration, integration of Eq. (8) (Fig. 3) yields a resultant force (per unit thickness):

$$F = \int_0^a p(x)dx \quad ,$$

$$\equiv - \left(\frac{6\eta\rho a^4}{h_m^3 \sigma_y Erb}\right)\left[\frac{a + 2rb}{a + rb}\right] K_{eff} \dot{K}_{eff} \quad , \tag{11}$$

which acts at a distance 3a/4 from the mouth of the fatigue crack.

The approximate stress intensity due to the presence of these concentrated forces can now be estimated, using:[14]

$$K^* = \frac{2Q}{\sqrt{\pi a}} F \quad , \tag{12}$$

where

$$Q = \frac{g(\xi)}{\sqrt{1 - \xi^2}}$$

and $$g(\xi) = 1.2945 - 0.2945\xi - 0.3912\xi^2 + 0.3912\xi^3 + 0.7685\xi^4 - 0.7685\xi^5 - 0.9942\xi^6 + 0.5094\xi^8 + 0.5094\xi^9.$$

For full penetration in the edge crack configuration, $\xi = 3/4$ and $Q = 1.58$. Thus the fluid-induced stress intensity factor becomes:

$$K^*(t) = \frac{-19\eta\rho a^4}{\sigma_y Erb\, h_m^3 \sqrt{\pi a}} \left[\frac{a + 2rb}{a + rb}\right] K_{eff} \dot{K}_{eff} \quad . \tag{13}$$

3.4 Effective Stress Intensity Range

Estimation of the effective stress intensities, $K_{eff}(t)$, during the fatigue cycle in the presence of viscous fluid-induced crack closure now involves superposition of the stress intensity due to the

fluid, $K^*(t)$, and the applied stress intensity, $K(t)$ (Fig. 5):

$$K_{eff}(t) \equiv K(t) + K^*(t)$$

$$= K_m + \frac{\Delta K}{2} \sin \omega t + \frac{2Q}{\sqrt{\pi a}} F(t) \quad , \tag{14}$$

where $K_m = 1/2(K_{max} + K_{min})$ and ω is the angular frequency.

For **full penetration** Eqs. (13) and (14) yield a differential equation in $K_{eff}(t)$:

$$\lambda \frac{\dot{K}_{eff}(t)}{K^5_{eff}(t)} + K_{eff}(t) = K_m + \frac{\Delta K}{2} \sin \omega t \quad . \tag{15}$$

where

$$\lambda = \frac{96\ Q\eta\rho(\sigma_y\ Erb)^2(\bar{a} + 2rb)a^4}{(\bar{a} + rb)^4(\pi a)^{\frac{1}{2}}}$$

The analogous solution for **partial penetration** is:

$$\lambda'[\int_0^t K^2_{eff}(t)]^{3/2} \frac{\dot{K}_{eff}(t)}{K^5_{eff}(t)} + K_{eff}(t) = K_m + \frac{\Delta K}{2} \sin \omega t \quad , \tag{16}$$

with

$$\lambda' = 1.54Q \left[\frac{\gamma^3 \cos^3\beta\ \sigma_y\ Erb}{\pi a(\bar{a} + 2rb)\eta\rho} \right]^{\frac{1}{2}} \quad ,$$

where Q is given by Eq. (12) with $\xi = d/2a$.

Solutions to Eqs. (15) and (16) are obtained numerically, using Newton's iterative method to linearize terms and then employing an implicit finite difference scheme to solve the resulting non-linear differential equations. Solutions were obtained relevant to the experimental room temperature fatigue crack propagation behavior of ASTM A542 Class 3 steel tested with compact specimens in silicone and paraffin oils (Table I).[3] In addition, based on approximate measurements of contact angle between the oils and the fracture surface, the wetting angle is taken to be of the order of 10°. The rotational factor r, is assigned a value of 0.4, which is typical for a 12.7 mm 1-T compact specimen of this grade of steel.[19]

4. RESULTS

Values of $K^{*}(t)$ are computed (Eq. (1), Fig. 5), and estimates of ΔK_{eff} (based solely on contributions from fluid-induced closure) are then derived using applied stress intensities K(t) and the values of K_q and K_p at maximum and minimum applied load, respectively. Solutions are obtained at two nominal ΔK ranges of 10 and 20 $MPa\sqrt{m}$ at two load ratios of R = 0.05 and 0.75 for tests in 25 and 75 cS paraffin oils and 5, 1000, 12500 and 60000 cS silicone oils. A crack length of 20 mm and a cyclic frequency of 50 Hz are considered for all cases, except where the specific role of varying crack length and frequency are examined.

From Eqs. (15) and (16), the variation in $K_{eff}(t)$ must be slightly out of phase with $K(t)$, as shown in Fig. 5. By considering peak values, computed estimates of K_q, K_p and hence ΔK_{eff} are shown in Figs. 6 to 8 and the relevant data listed in Table I. In Fig. 6, computed values of K_q and K_p are plotted as a function of kinematic viscosity ($0 < \eta < 10^7$ cS), assuming full penetration of fluid into the crack (Eq. (15)). It is apparent that both the effective maximum and minimum stress intensities, K_q and K_p, tend towards the mean stress intensity, K_m, with increasing viscosity, consistent with the fact that as $\eta \to \infty$ (i.e., a rigid wedge), ΔK_{eff} must tend to zero. However, although the increase in K_p is fairly sharp, the corresponding decay in K_q is slight (i.e., < 1 MPa$\sqrt{m}$ at ΔK = 10 or 20 MPa$\sqrt{m}$ for $\eta < 10^5$ cS). Thus, for the oils studied, the effective "saturation" value of K^*_{max} will not be of the order of K_{max} but rather of K_m, such that the maximum extent of closure will be approximately $\Delta K_{eff} \sim 0.5\ \Delta K$.

In Fig. 7, the corresponding K_q and K_p values based on solutions to the partial penetration model (Eq. (16)) are plotted as a function of the normalized penetration distance, $d/\bar{a}$, and are compared to values determined from the full penetration model (Eq. (15)). Comparison of the two solutions as $d/\bar{a} \to 1$ shows reasonable agreement, with the solutions for K_q and K_p becoming identical for kinematic viscosities above 1000 cS.

Several points are worthy of note from this analysis. First, no significant fluid pressure is generated at R = 0.75, where the crack

opening displacements are relatively much larger. However, at a low load ratio of R = 0.05 (Fig. 7), aside from the small change in K_q, K_p can be seen to increase monotonically with increasing oil penetration ($d/\bar{a}$) and increasing oil viscosity (η). Furthermore, the development of a significant stress intensity, $K^*_{max} = K_q + K_p$, requires a smaller extent of penetration for the higher viscosity oils. Corresponding values of ΔK_{eff} at ΔK = 10 and 20 MPa$\sqrt{m}$ (R = 0.05), derived from Fig. 7, are shown in Fig. 8 as a function of $d/\bar{a}$, and again indicate a maximum extent of fluid-induced closure of $\Delta K_{eff} \sim 0.5\ \Delta K$.

The influence of fatigue crack length ($\bar{a} = a - a_o$) on the development of K^* is shown in Fig. 9 based on solutions to the full penetration model. K^*_{max} values can be seen to decrease with decreasing crack length, but only at the smaller crack sizes. This indicates that the extent of viscous fluid-induced crack closure diminishes for small cracks, similar to behavior reported for other mechanisms of crack closure.[2,20]

With regards to capillary flow of fluid into the crack, the normalized penetration distance, $d/\bar{a}$ (Fig. 10), is, as expected, largest for the lowest viscosity oils. Specifically at low load ratios, complete penetration of the lower viscosity oils (η < 75 cS) to the crack tip is apparent within 200 s (10^4 cycles) at ΔK = 10 MPa$\sqrt{m}$ and 40 s (2000 cycles) at ΔK = 20 MPa$\sqrt{m}$.

5. DISCUSSION

The predictions from the full and partial penetration models for viscous fluid-induced crack closure, shown in Figs. 6 to 10, indicate that although such closure should progressively increase with increasing viscosity, the values of K^* developed will be kinetically limited by the penetration of the viscous fluid at high viscosities. Thus prediction of the magnitude of the closure effect is achieved by comparing the relative magnitude of the average, steady-state, rate of oil penetration, $\langle \dot{d} \rangle$, from Eq. (2), to the rate of crack extension, $\dot{a}$, from Fig. 1 and ref. 3, specifically for tests at R = 0.05 and 50 Hz at ΔK = 10 and 20 MP$\sqrt{m}$ (Fig. 11). It is apparent that penetration rates for the lower viscosity oils (i.e., $\eta \lesssim 75$ cS) are far in excess of growth rates, by at least two orders of magnitude, such that full penetration can be safely assumed. However, for the higher viscosity oils (i.e., $\eta \gtrsim 12500$ cS), the penetration and growth rates are comparable and the assumption of full penetration becomes suspect. Consequently, predictions of $d/\bar{a}$, K^* and ΔK_{eff} for a crack length of 20 mm in a compact geometry (relevant to the experimental data for A542 Class 3 steel in Part I (Fig. 1)), reveal a general trend for the least closure to be generated with the highest viscosity fluids (Table I).

A comparison of ΔK_{eff} values, assuming closure due only to hydrodynamic wedging, with the experimental data for A542 Class 3 steel (e.g., Fig. 1) is shown in Fig. 12. In this figure, the crack

growth rates in oil, $(da/dN)_{oil}$, are plotted for nominal ΔK values of 10 and 20 MPa$\sqrt{m}$ at R = 0.05 as a function of the kinematic viscosity of the oils. The predicted values of ΔK_{eff} from Table I are given in parentheses by each datum point. It is apparent that although the variation in both measured growth rates and predicted ΔK_{eff} values is narrow, **in general** the highest growth rates at each ΔK correspond to the highest predicted effective stress intensity ranges. Thus, without any recourse to the use of adjustable parameters, the current quantitative analysis of viscous fluid-induced crack closure provides feasible estimates of the closure stress intensities and ΔK_{eff} for crack growth in viscous fluids.

As a further evaluation of the above analyses, the effect of varying frequency, specifically from 50 to 5 Hz, is examined in the 25 cS paraffin oil. Based in Eq. (2), the penetration rates of the fluid at ΔK = 10 and 20 MPa$\sqrt{m}$ (R = 0.05) are marginally faster at 5 Hz (Fig. 13). These results indicate full penetration of the 20 mm crack by 25 cS paraffin oil within a minute at either frequency. The corresponding development of a resultant stress intensity, K^*_{max} as a function of fluid penetration, $d/\bar{a}$, is shown for the two frequencies, at ΔK = 10 and 20 MPa$\sqrt{m}$, in Fig. 14. It is apparent that the slower closing velocity of the crack walls ($\dot{\theta}$) at 5 Hz results in a lower fluid pressure, lower K^*_{max} values and hence less fluid-induced closure. Thus, due to less closure at the lower frequency, crack growth rates in the 25 cS paraffin oil should be faster at 5 Hz compared to 50 Hz. Such predictions were confirmed by experimental

growth rate measurements on the A542-3 steel between 10^{-7} and 10^{-4} mm/cycle (R = 0.05), where propagation rates are increased by up to a factor of 5 at the lower frequency (Fig. 15). Model predictions of K^*_{max} and ΔK_{eff} (Table I) are compared with experimental growth rate results in Fig. 12.

Finally, it is pertinent to emphasize the assumptions implicit in the current analysis. First, the kinetic analysis is based on capillary flow between smooth parallel-sided plates, rather than the penetration of a viscous fluid into a microstructurally-rough crack under cyclic loading. Second, changes in the internal fluid pressure distribution due to cavitation and variations in viscosity with pressure have been ignored. Furthermore, the comparison of the model predictions with experimental fatigue crack growth results in oils (e.g., Fig. 12) assumes the absence of active constituents in the oils and that the primary source of closure is due to the fluid pressure. In view of the extensive **in situ** dehumidification procedures,[3] it would seem reasonable to assume that the oils are effectively inert.

6. CONCLUDING REMARKS

A model for fatigue crack closure induced by the presence of viscous fluids has been developed based on considerations of capillary flow, hydrodynamics and fracture mechanics. The model, unlike previous analyses,[9,10] considers both partial and full

penetration of fluid within the crack, and the resulting predictions of effective stress intensities are consistent with experimental growth rate data in a pressure vessel steel (σ_y = 500 MPa) tested in a range of oils.[3] The analysis indicates that the extent of the fluid-induced closure can be influenced by viscosity and other physical properties of the fluid, applied stress intensities, frequency, load ratio and yield strength. However, the expected trend is difficult to predict since the development of an internal fluid pressure, which is **increased** by increasing viscosity, must be balanced by the ability of the oil to penetrate the crack, which is **decreased** with increasing viscosity. It is presumably this mutual competition between the relative dominance of the hydrodynamic and kinetic factors which has led to the conflicting observations of this effect in the past literature.[4-11]

Finally, it is noted that although values of the stress intensity due to the fluid pressure, K^*_{max}, should tend to K_{max} (i.e., $\Delta K_{eff} \rightarrow 0$) as $\eta \rightarrow \infty$, for the majority of viscous fluids (i.e., $\eta < 10^5$ cS) values of K^*_{max} will tend to saturate close to the mean stress intensity, K_m, of the fatigue cycle due to the minimal change in K_q. This suggests that the maximum extent of closure will be of the order of K_{cl}/K_{max} of 0.5. Thus, the hydrodynamic wedge mechanism must be regarded as a less potent mechanism of closure, compared to other sources, such as induced by cyclic plasticity, corrosion debris or fracture surface roughness, where considerably higher K_{cl}/K_{max} values are possible.[1,2,21,22] The process is, however, similar to

other closure mechanisms in that the magnitude of the effect is significantly reduced at high load ratios, and with decreasing crack length (Fig. 9). As with closure mechanisms in general, the latter suggests an R-curve effect, of increasing applied driving force to maintain constant crack advance. This is particularly significant to the problem of short fatigue cracks since, at the same nominal ΔK value, the short crack will experience a higher ΔK_{eff}, due to a lesser influence of closure, and therefore may be expected to propagate at a faster rate compared to the equivalent long crack. Such behavior has been widely reported in the presence of other mechanisms of closure.[20]

Acknowledgements - The work, which was performed in partial fulfillment of the M.S. degree of J.-L. Tzou, was supported by the Director, Office of Energy Research, Office of Basic Energy Sciences, Materials Science Division of the U.S. Department of Energy under Contract No. DE-AC03-76SF00098. Thanks are due to Professors S. Suresh and J. W. Evans for helpful discussions, and Madeleine Penton for typing the manuscript.

NOMENCLATURE

a	crack length
$\bar{a}$	fatigue crack length (= a for edge crack geometry and $(a - a_o)$ for compact tension geometry)
a_o	notch length (compact tension geometry)
$\dot{a}$	crack velocity, with respect to time
b	uncracked ligament $(W - a)$
B	test piece thickness
d	penetration distance of viscous fluid into crack
da/dN	fatigue crack growth rate per cycle
E	Young's modulus
f	dimensionless function of a/W in Eq. (3)
F	resultant force/unit thickness due to oil pressure
g	dimensionless function defined in Eq. (12)
$\langle h \rangle$	average crack opening width
h_m	fatigue crack mouth opening width (CMOD)
h_δ	crack tip opening width (CTOD)
K	linear elastic stress intensity factor in Mode I
K_{eff}	instantaneous near tip (effective) stress intensity
K_{cl}	stress intensity to cause closure of the crack
K_m	mean stress intensity $(K_{max} - K_{min})/2$
K_{max}	maximum stress intensity during fatigue cycle
K_{min}	minimum stress intensity during fatigue cycle

K_p	increase in K_{min} due to hydrodynamic action of fluid
K_q	decrease in K_{max} due to hydrodynamic action of fluid
K^*	stress intensity due to hydrodynamic action of viscous fluid inside the crack during cyclic loading
K^*_{max}	maximum value of K^*, evaluated at peak loads ($K_q + K_p$)
ΔK	alternating stress intensity ($K_{max} - K_{min}$)
ΔK_{eff}	effective stress intensity range ($K_{max} - K_{cl}$)
N	number of cycles
P	applied load
p(x)	pressure distribution due to fluid as a function of distance x along crack
Q	geometry factor in expressions for K^* (Eq. (12))
r	non-dimensional rotational factor
R	load ratio (K_{min}/K_{max})
t	time
W	test piece width
x	distance coordinate along crack length, measured from crack mouth
β	wetting angle between fluid and crack walls
γ	surface tension of fluid
η	kinematic viscosity
λ, λ'	functions defined in Eqs. (15) and (16), respectively
ρ	density of fluid
σ_y	tensile yield strength
ξ	dummy variable in Eq. (12)

$\dot{\theta}$	angular closing velocity of crack walls
ω	angular frequency

REFERENCES

1. W. Elber: in Damage Tolerance in Aircraft Structures, ASTM STP 486, 1971, p. 230.
2. S. Suresh and R. O. Ritchie: in Concepts of Fatigue Crack Growth Thresholds, D. L. Davidson and S. Suresh, eds., TMS-AIME, Warrendale, PA, 1984, in press (Lawrence Berkeley Laboratory Report No. LBL-16263, Sept. 1983).
3. J.-L. Tzou, S. Suresh and R. O. Ritchie: (Part I): Acta Met., 1984, in review (Lawrence Berkeley Laboratory Report No. LBL-16028, Dec. 1983).
4. S. Way: J. Appl. Mech., Trans. ASME Series E, 1935, vol. 2, p. A49.
5. J. B. Martin and A. Cameron: J. Mech. Eng. Sci., 1961, vol. 3, p. 148.
6. F. G. Rounds: ASLE Trans., 1962, vol. 5, p. 172.
7. G. D. Galvin and H. Naylor: Proc. Instn. Mech. Engrs. 1964-65, vol. 179, p. 857.
8. W. E. Littermann, R. L. Widner, J. O. Wolfe, and J. D. Stover: J. Lubric. Tech., Trans. ASME Series F, 1968, vol. 90, p. 89.
9. K. Endo, T. Okada, and T. Hariya: Bull. JSME, 1972, vol. 15, p. 439.
10. K. Endo, T. Okada, K. Komai, and M. Kiyoto: Bull. JSME, 1972, vol. 15, p. 1316.
11. F. G. Rounds: ASLE Trans., 1977, vol. 20, p. 115.

12. S. Newman: J. Colloid Interface Sci., 1968, vol. 26, p. 209.

13. H. Tada, P. C. Paris, and G. R. Irwin: in The Stress Analysis of Cracks Handbook, Del Research Corp., Hellertown, PA, 1973.

14. G. C. Sih: in Handbook of Stress Intensity Factors, Lehigh Univ. Press, Bethlehem, PA, 1973.

15. A. Turnbull: Corrosion Science, 1982, vol. 22, p. 877.

16. C. F. Shih: J. Mech. Phys. Solids, 1981, vol. 21, p. 305.

17. C. C. Veerman and T. Muller: Eng. Fract. Mech., 1972, vol. 4, p. 25.

18. D. D. Fuller: in Theory and Practice of Lubrication for Engineers, Wiley, New York, NY, 1956, p. 135.

19. T. Ingham, G. R. Egan, and D. Elliott: in Practical Applications of Fracture Mechanics to Pressure Vessel Technology (1st Int. Conf. Proc.), R. W. Nichols, ed., Instit. Mech. Eng., London, 1971.

20. S. Suresh and R. O. Ritchie: Int. Met. Reviews, 1984, vol. 25, in press (University of California, Berkeley, Report No. UCB/RP/83/A1014, June 1983).

21. S. Suresh and R. O. Ritchie: Scripta Met., 1983, vol. 17, p. 575.

22. S. Suresh and R. O. Ritchie: Metall. Trans. A, 1982, vol. 13A, p. 1627.

Table I: Estimates for the Magnitude of Viscous Fluid Induced Crack Closure for the Compact Specimen

(A) For $\Delta K = 10\ MPa\sqrt{m}$, R = 0.05, a = 20 mm

Oil	η (cS)	γ (dyne/cm)	ρ (g/cm^3)	$d/\bar{a}$	K^*_{max} $(K_p + K_q)$ (MPa$\sqrt{m}$)	ΔK_{eff} (MPa$\sqrt{m}$)
silicone	5	19.7	0.920	1	4.7-5	5-5.3
	1,000	21.2	0.970	1	5.7	4.3
	12,500	21.5	0.975	0.10	4.9	5.1
	60,000	21.5	0.975	0.03	4.5	5.5
paraffin	25	35.0	0.870	1	5.4	4.6
	75	36.0	0.890	1	5.5	4.5
	(5 Hz) 25	35.0	0.870	1	3.6	6.4

(B) For $\Delta K = 20\ MPa\sqrt{m}$, R = 0.05, a = 20 mm

Oil	η (cS)	γ (dyne/cm)	ρ (g/cm^3)	$d/\bar{a}$	K^*_{max} $(K_p + K_q)$ (MPa$\sqrt{m}$)	ΔK_{eff} (MPa$\sqrt{m}$)
silicone	5	19.7	0.920	1	4.7-5.5	14.5-15.4
	1,000	21.2	0.971	0.50	9.0	11.0
	12,500	21.5	0.975	0.15	7.6	12.4
	60,000	21.5	0.975	0.05	5.8	14.2
paraffin	25	35.0	0.870	1	6.6∿7.9	12.1∿13.4
	75	36.0	0.890	1	8.0∿9.3	10.7∿12.0
	(5 Hz) 25	35.0	0.870	1	3.6	16.4

Conditions

Room temperature

50 Hz frequency (sine wave), except where indicated

ASTM A542 Class 3 steel ($E = 2.1 \times 10^5$ MPa, $\sigma_y = 500$ MPa)

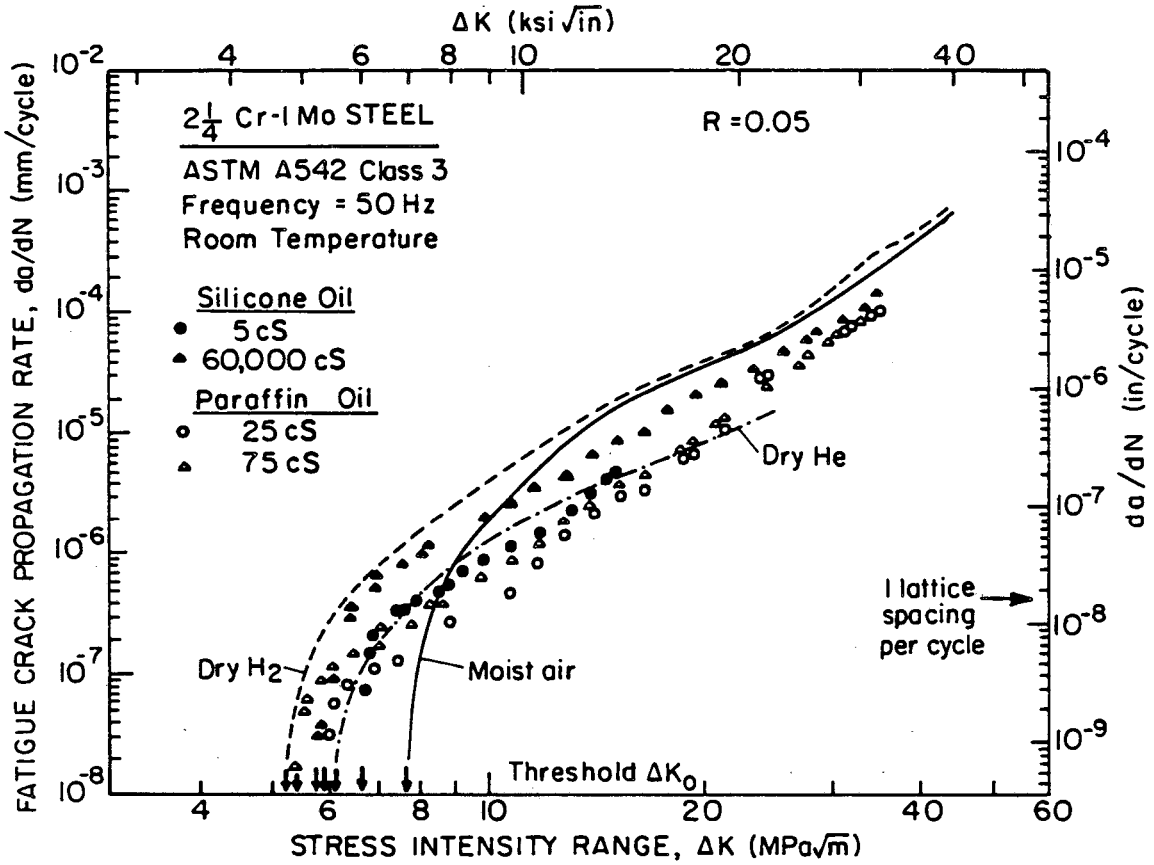

Fig. 1. Experimentally measured variation in fatigue crack propagation rates (da/dN) with nominal stress intensity range (ΔK) in bainitic 2¼Cr-1Mo steel tested at R = 0.05 (50 Hz) in silicone and paraffin oils, compared to results in moist air, dry helium and dry hydrogen gases (after ref. 3).

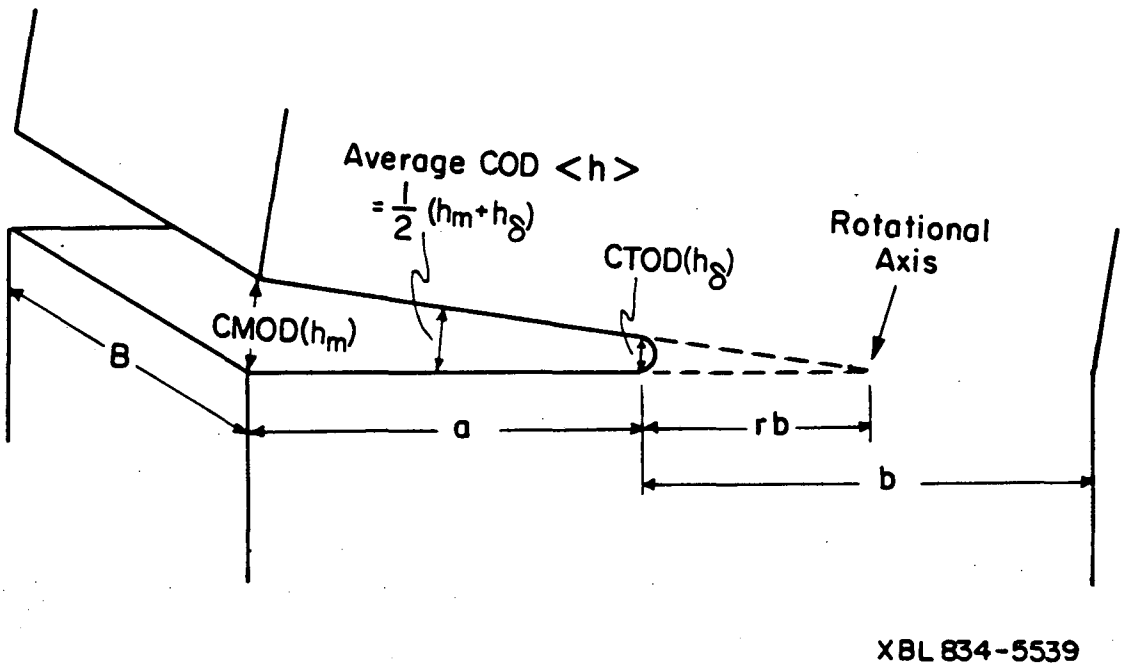

Fig. 2. Schematic illustration of idealized fatigue crack, showing definitions of the rotational axis and crack opening displacements.

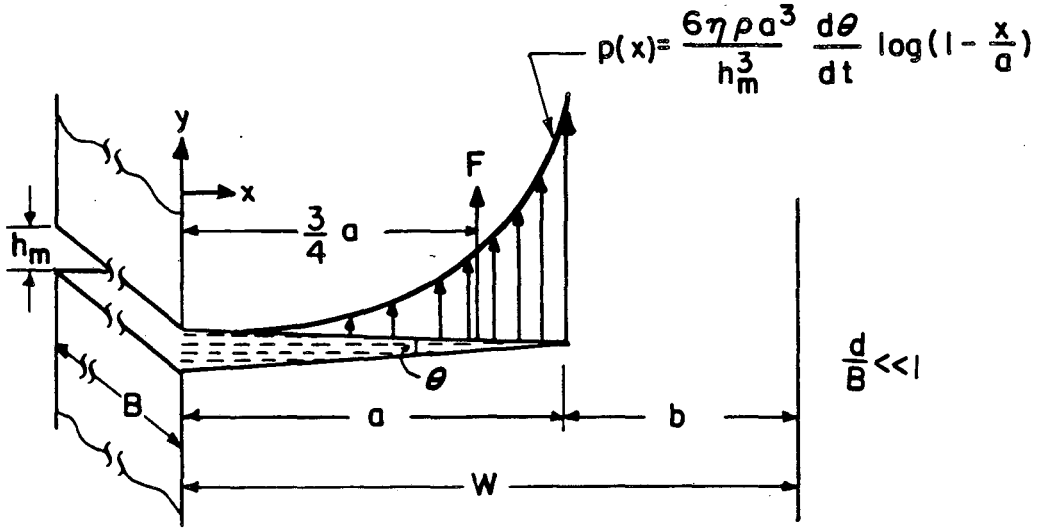

a) Arbitrary Edge Crack

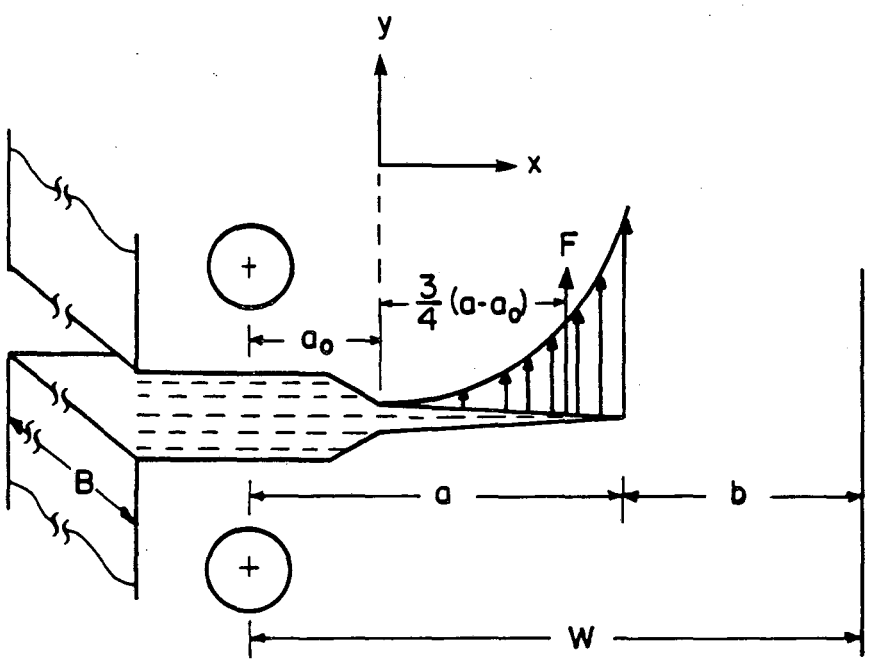

b) Crack in a C(T) Specimen

XBL 834-5537

Fig. 3. Schematic illustration of the internal pressure distribution p(x) and resultant concentration force (F) due to the full penetration of fluid inside the crack for a) edge crack and b) compact tension C(T) geometries.

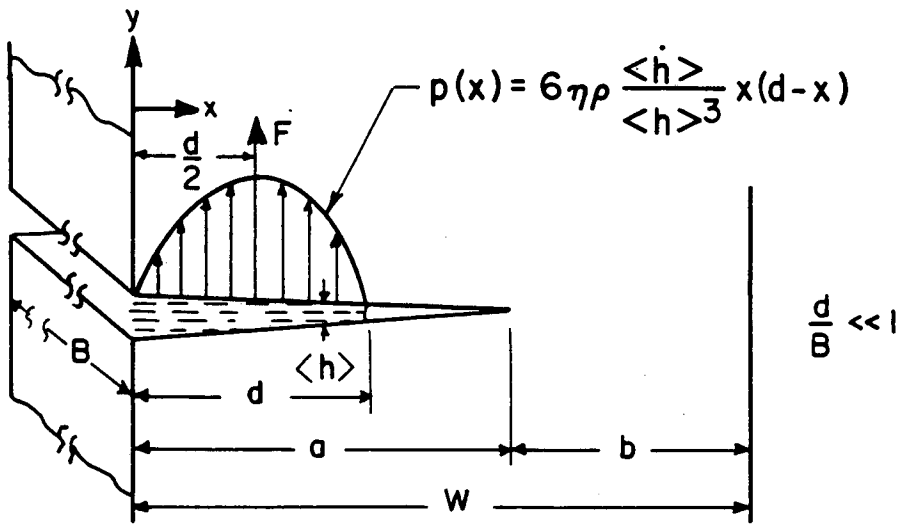

a) Arbitrary Edge Crack

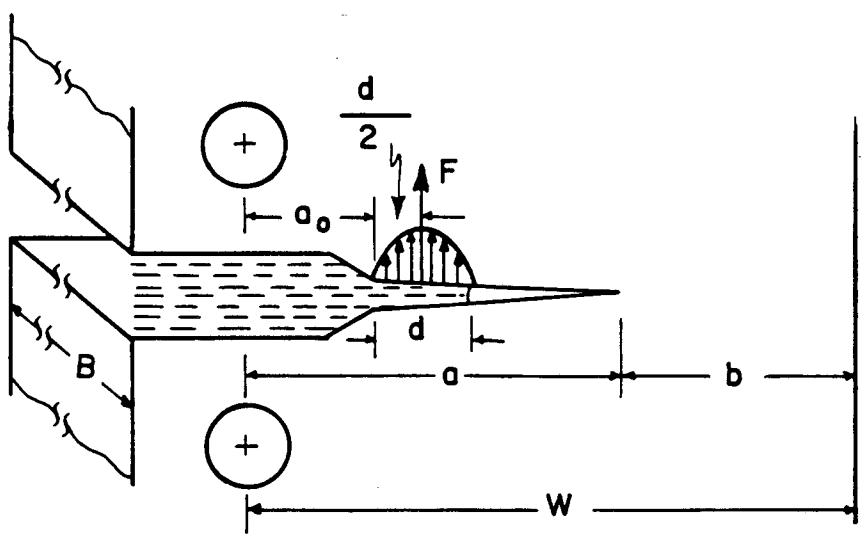

b) Crack in a C(T) Specimen

XBL 834-5540

Fig. 4. Schematic illustration of the internal pressure distribution p(x) and resultant concentration force (F) due to the partial penetration of fluid inside the crack for a) edge crack and b) compact tension C(T) geometries.

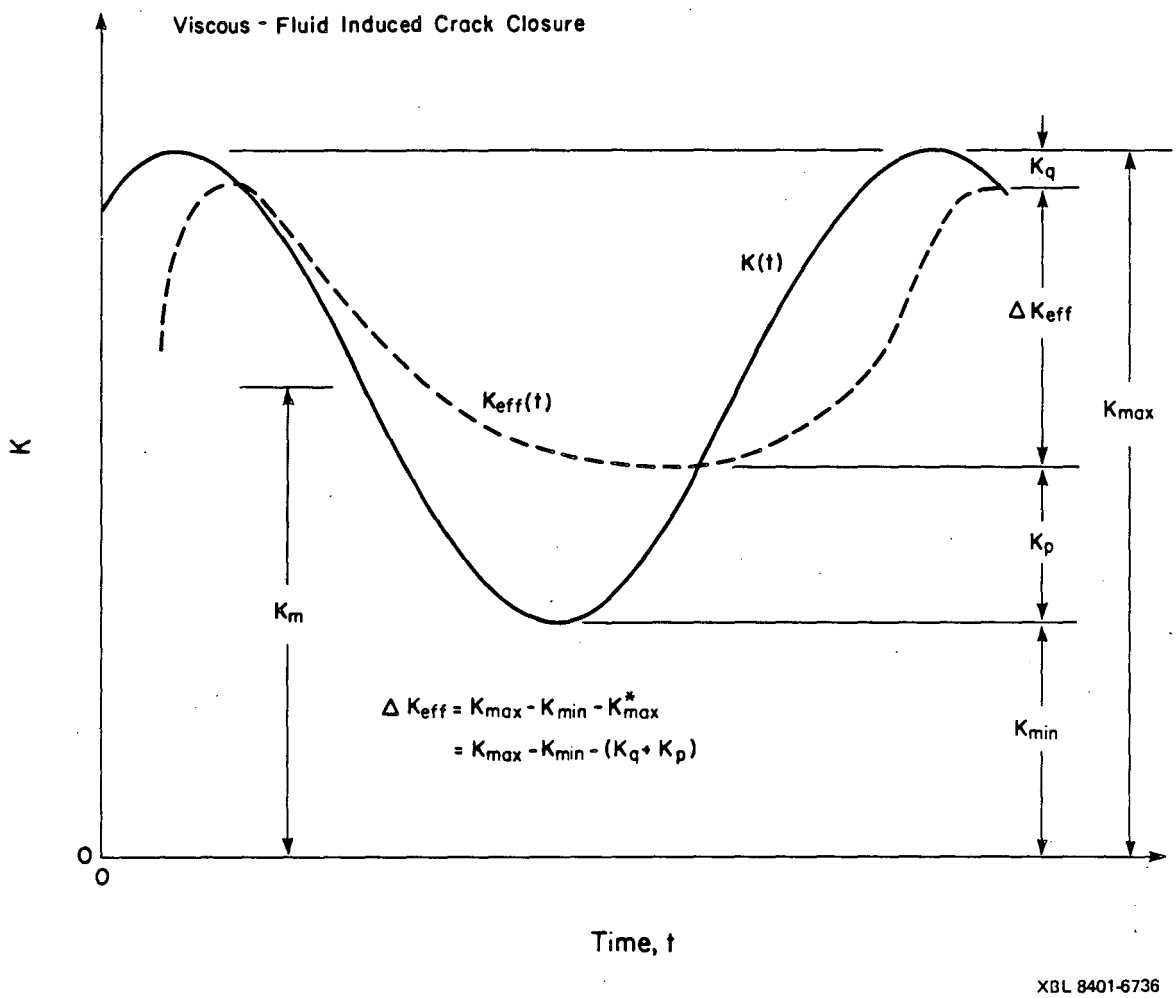

Fig. 5. Schematic illustration of the superposition of $K^*(t)$ values and nominal stress intensity $K(t)$ values over the fatigue cycle to yield effective stress intensity $K_{eff}(t)$ values actually experienced at the crack tip, assuming closure due only to viscous fluids. The maximum value of K^* is comprised of K_q, the effective maximum stress intensity, and K_p, the effective minimum stress intensity, due to the fluid pressure.

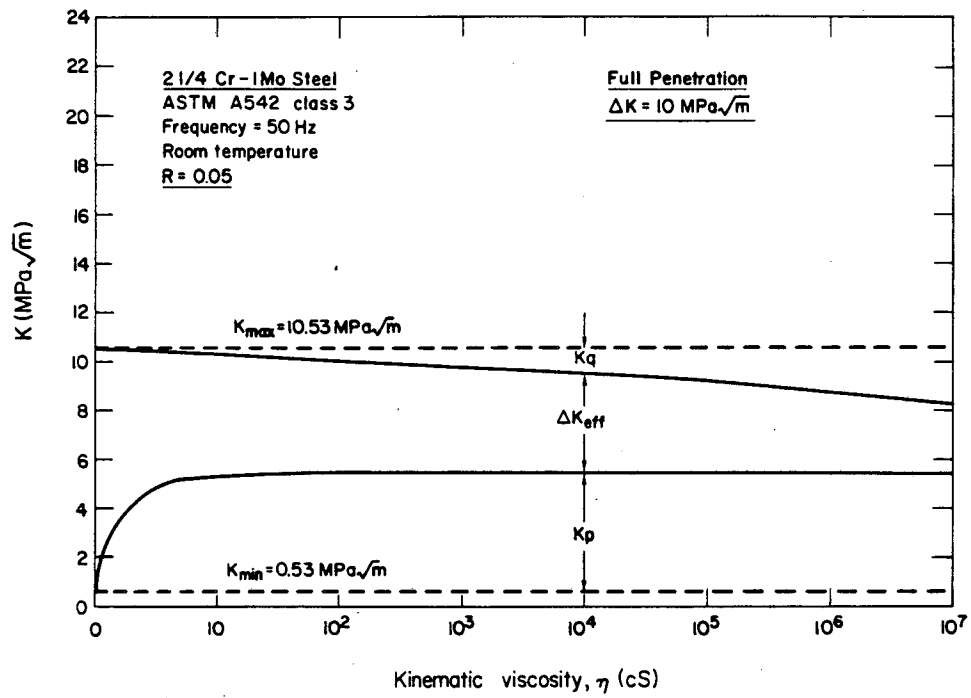

(a)

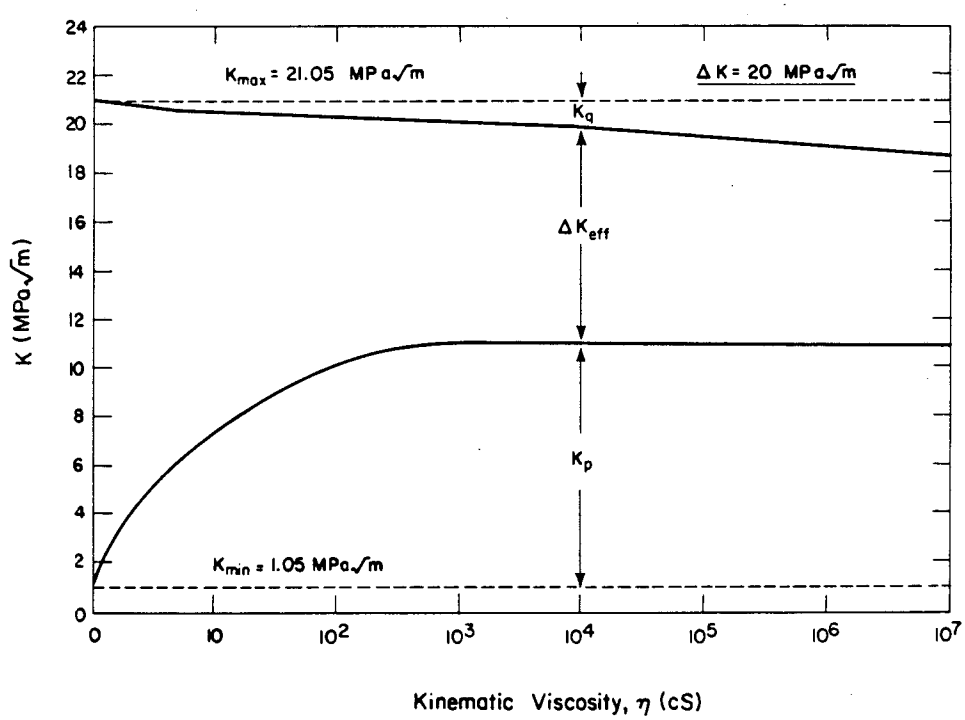

(b)

XBL 8401-6734

Fig. 6. Predicted values of the stress intensities due to fluid pressure, K_q and K_p, as a function of kinematic viscosity, η, for a) $\Delta K = 10$ MPa$\sqrt{m}$ and b) $\Delta K = 20$ MPa$\sqrt{m}$ at R = 0.05 (50 Hz). Predictions for a 20 mm crack in silicone and paraffin oils based on full penetration model ($d/\bar{a} = 1$) in Eq. (15).

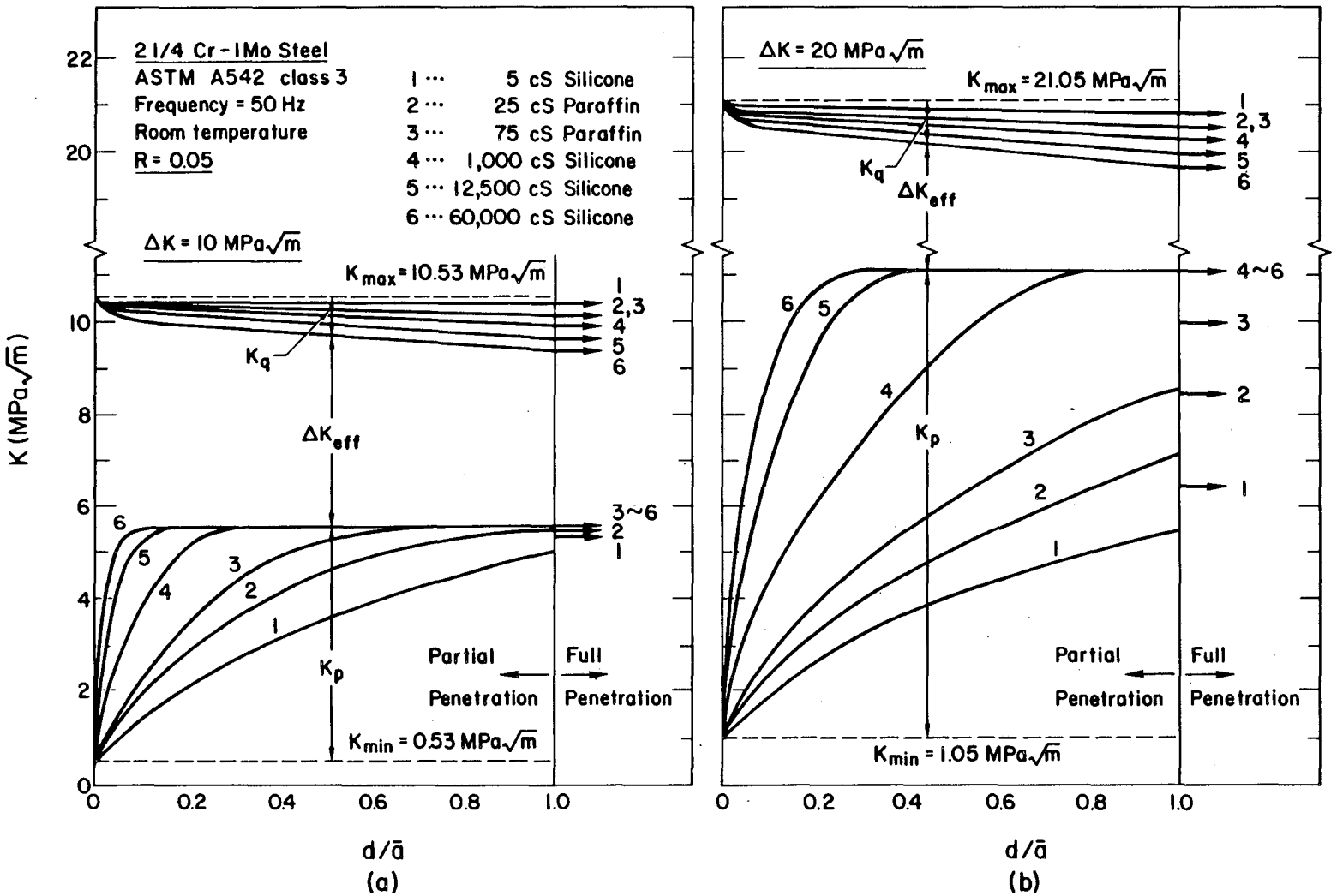

XBL 8401-6733

Fig. 7. Predicted values of the stress intensities due to fluid pressure, K_q and K_p, as a function of normalized fluid penetration distance, $d/\bar{a}$, for a) $\Delta K = 10$ MPa$\sqrt{m}$ and b) $\Delta K = 20$ MPa$\sqrt{m}$ at $R = 0.05$ (50 Hz). Predictions for a 20 mm crack in silicone and paraffin oils based on full penetration model ($d/\bar{a} = 1$) in Eq. (15) and partial penetration model ($d/\bar{a} < 1$) in Eq. (16).

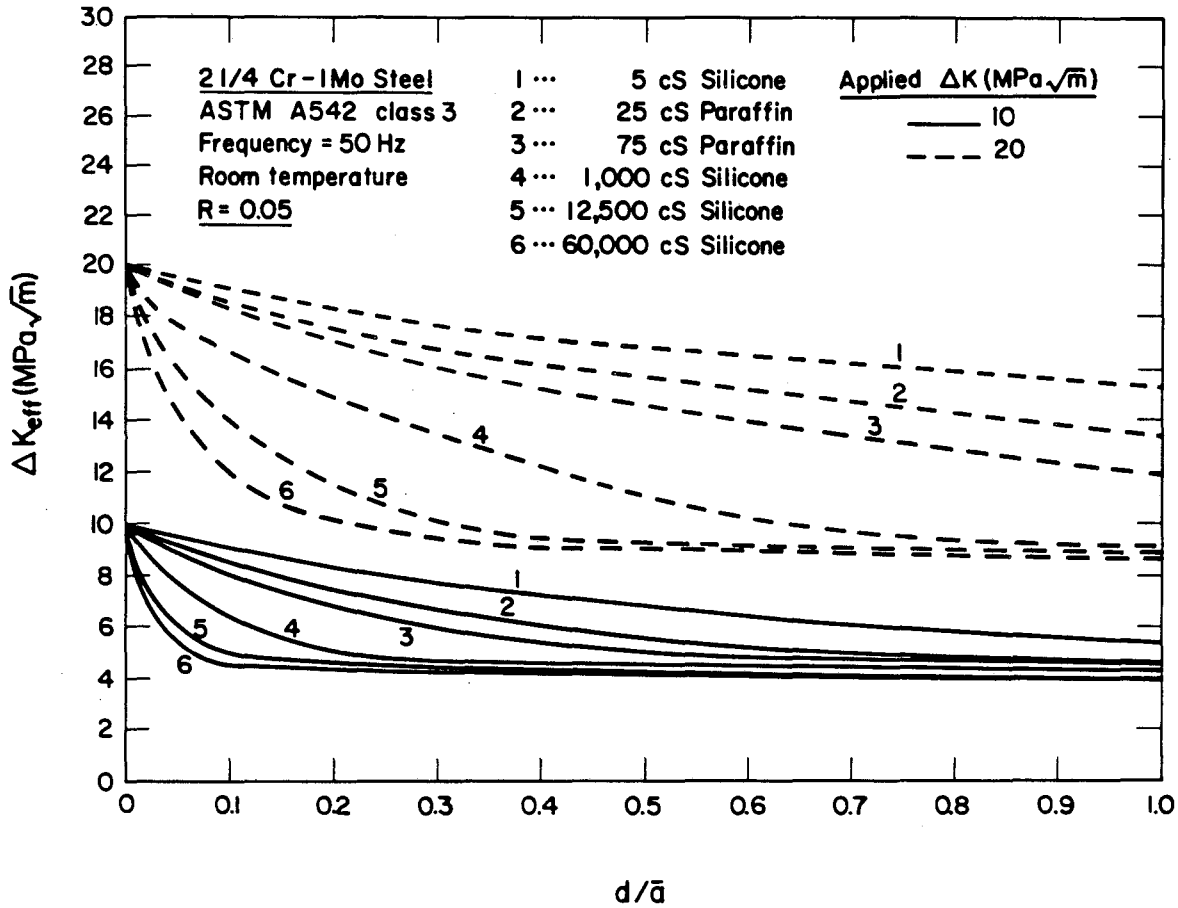

Fig. 8. Predicted variation in the effective stress intensity range, ΔK_{eff}, due to fluid-induced closure in silicone and paraffin oils, as a function of normalized penetration distance, $d/\bar{a}$, at ΔK = 10 MPa$\sqrt{m}$ (R = 0.05, 50 Hz). Predictions for a 20 mm crack based on partial penetration model (Eq. (16)).

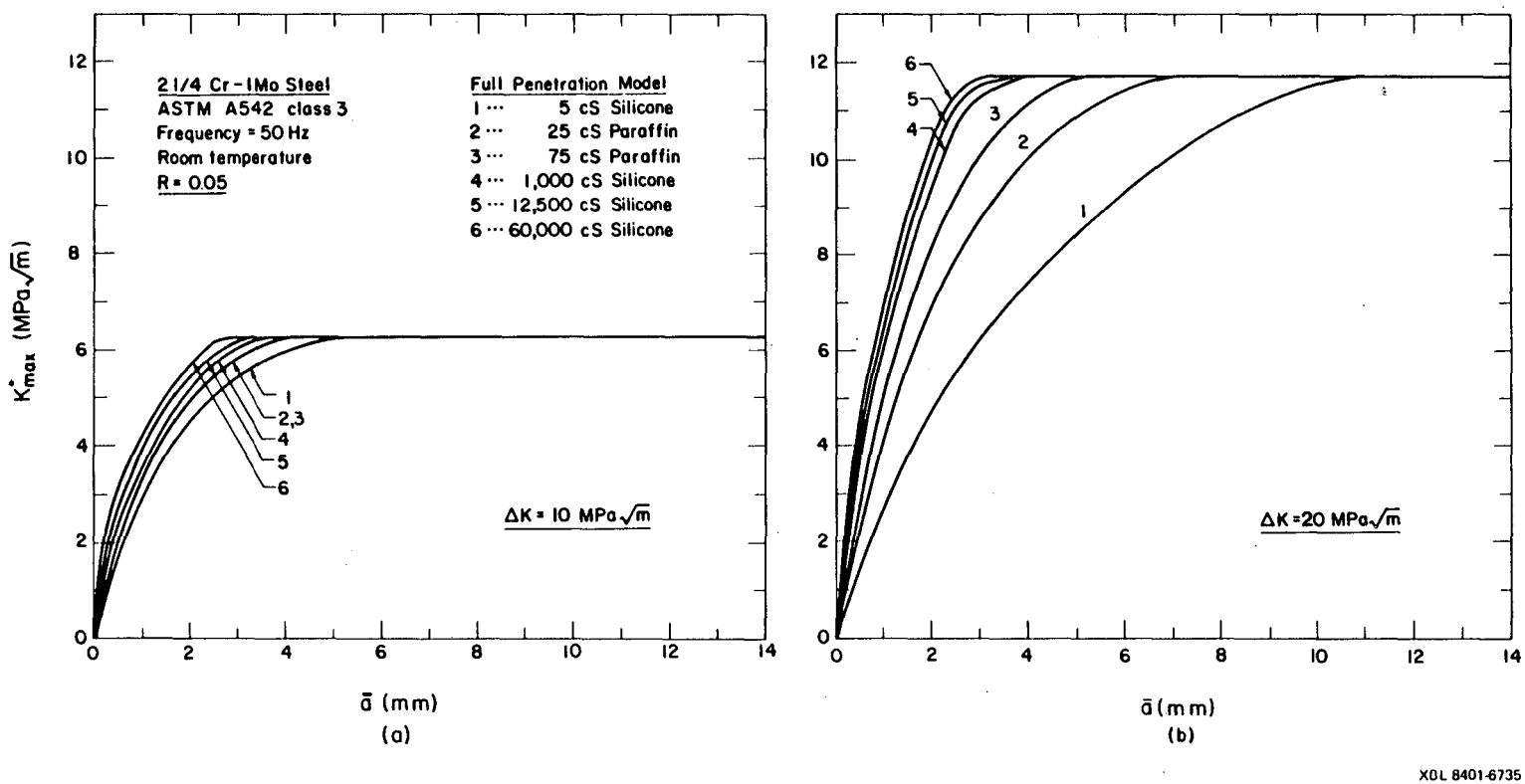

Fig. 9. Effect of crack size on predicted value of K^*_{max} ($\approx K_q + K_p$) at ΔK = 10 and 20 MPa$\sqrt{m}$ (R = 0.05, 50 Hz) based on full penetration model (Eq. (15)). Predictions for silicone and paraffin oils as a function of the fatigue crack length $\bar{a}$.

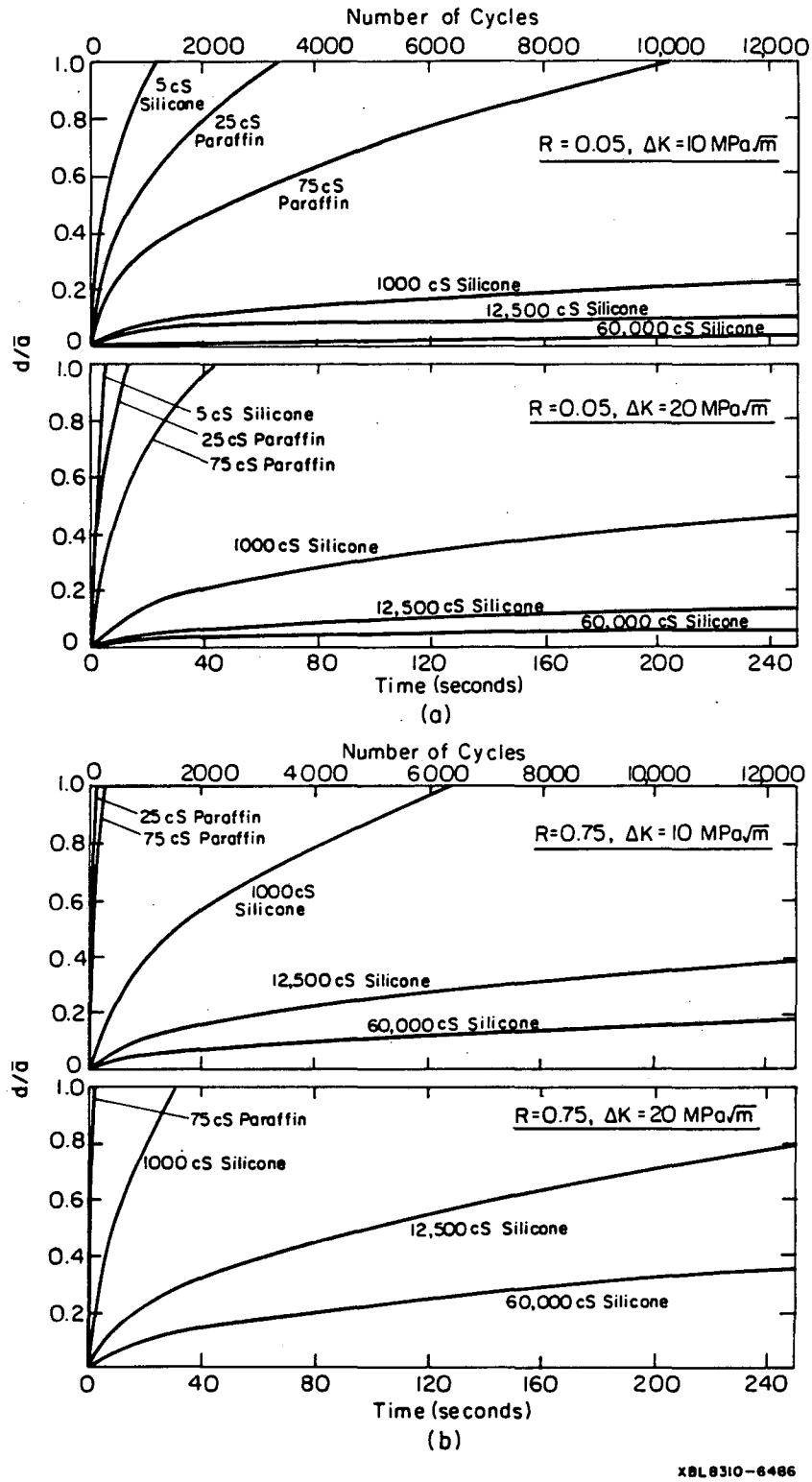

Fig. 10. Prediction of normalized fluid penetration rates ($d/\bar{a}$ vs. time) for paraffin and silicone oils based on capillary flow equations (Eq. (2)). Predictions for 20 mm crack tested at 50 Hz with ΔK = 10 and 20 MPa$\sqrt{m}$ at R = 0.05 and 0.75.

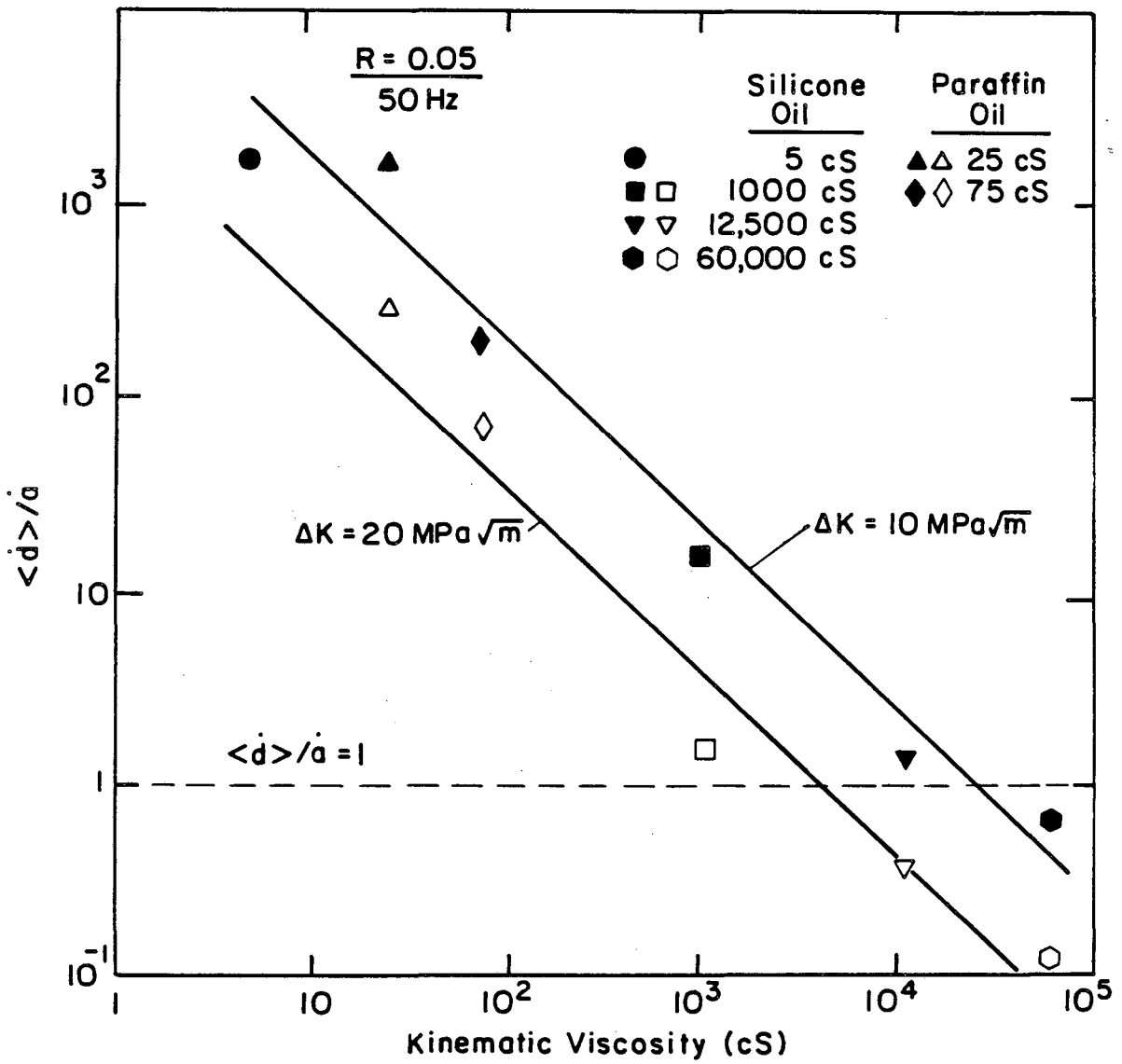

Fig. 11. Variation of the ratio of average fluid penetration rate (from Eq. (2)) to crack growth rate (from Fig. 1), $\langle\dot{d}\rangle/\dot{a}$, as a function of kinematic viscosity, η, for paraffin and silicone oils at ΔK = 10 and 20 MPa$\sqrt{m}$ (R = 0.05, 50 Hz).

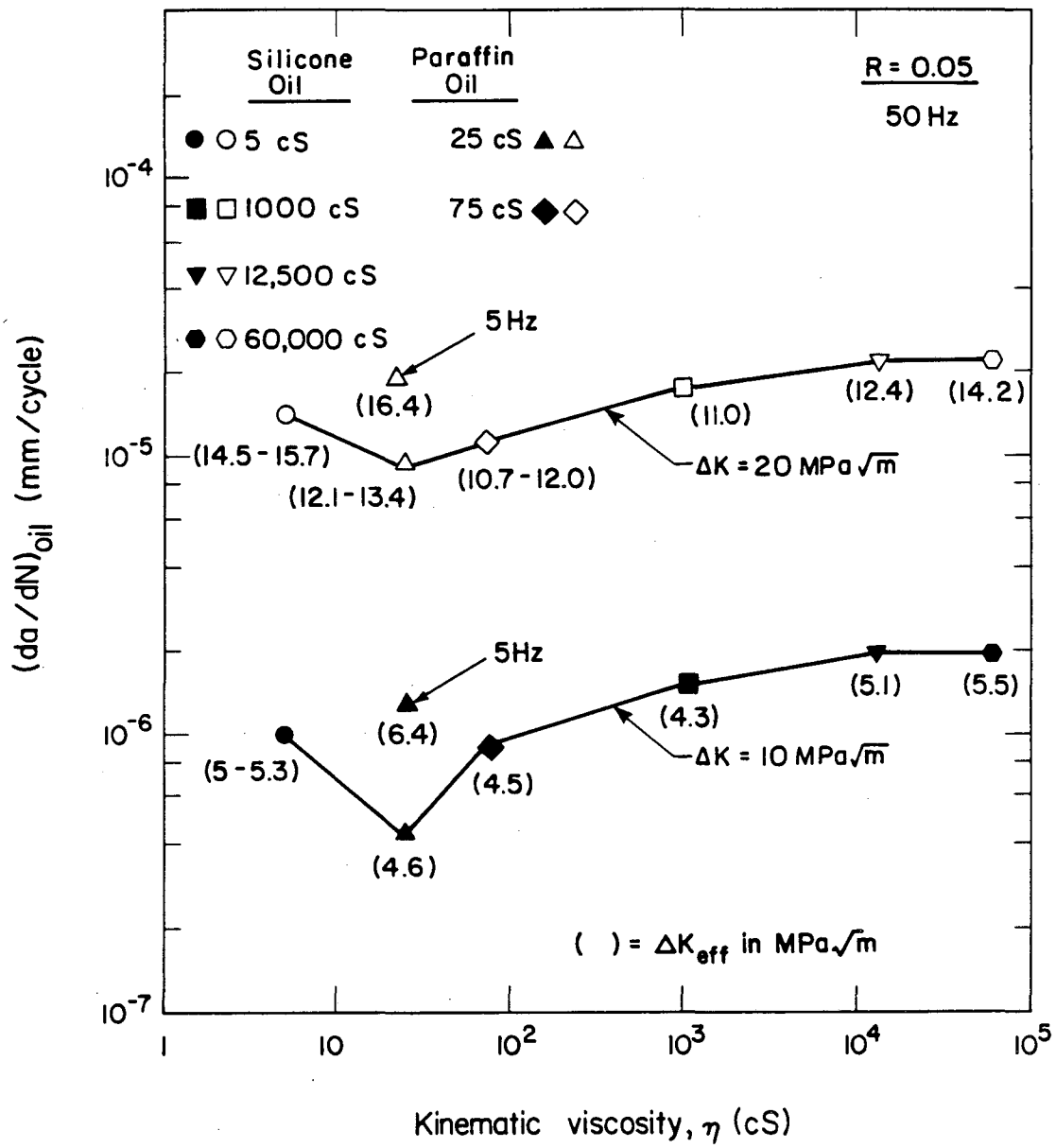

Fig. 12. Variation of fatigue crack propagation rate at ΔK = 10 and 20 MPa$\sqrt{m}$ (R = 0.05) with kinematic viscosity η of paraffin and silicone oils. Numbers in parentheses represent predictions of ΔK_{eff} in MPa$\sqrt{m}$ based on proposed model for fluid-induced crack closure (Eqs. (15) and (16)). Results for 50 Hz frequency except indicated data points for 5 Hz.

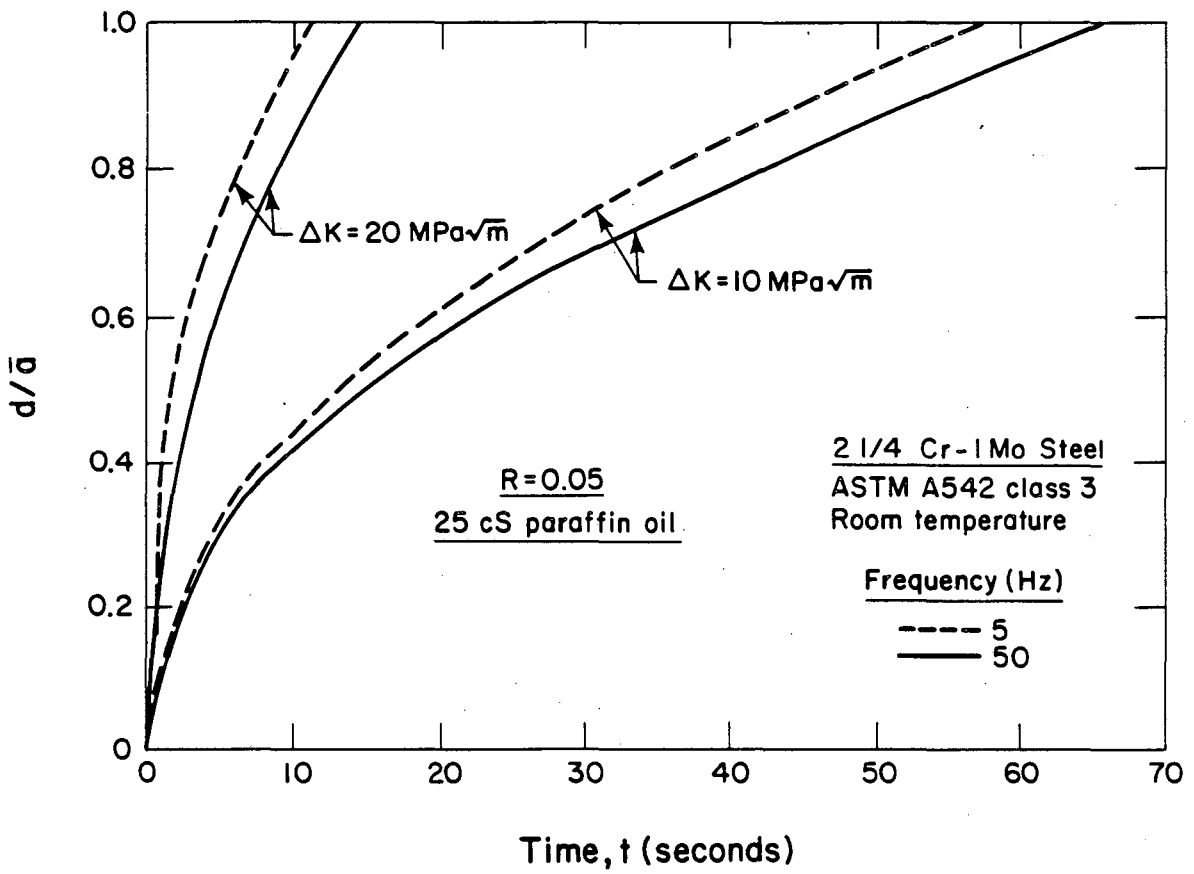

Fig. 13. Predicted effect of frequency on normalized fluid penetration rates ($d/\bar{a}$ vs. time) for 25 cS paraffin oil tested at ΔK = 10 and 20 MPa$\sqrt{m}$ (R = 0.05). Predictions for 20 mm crack from Eq. (2) at 5 and 50 Hz.

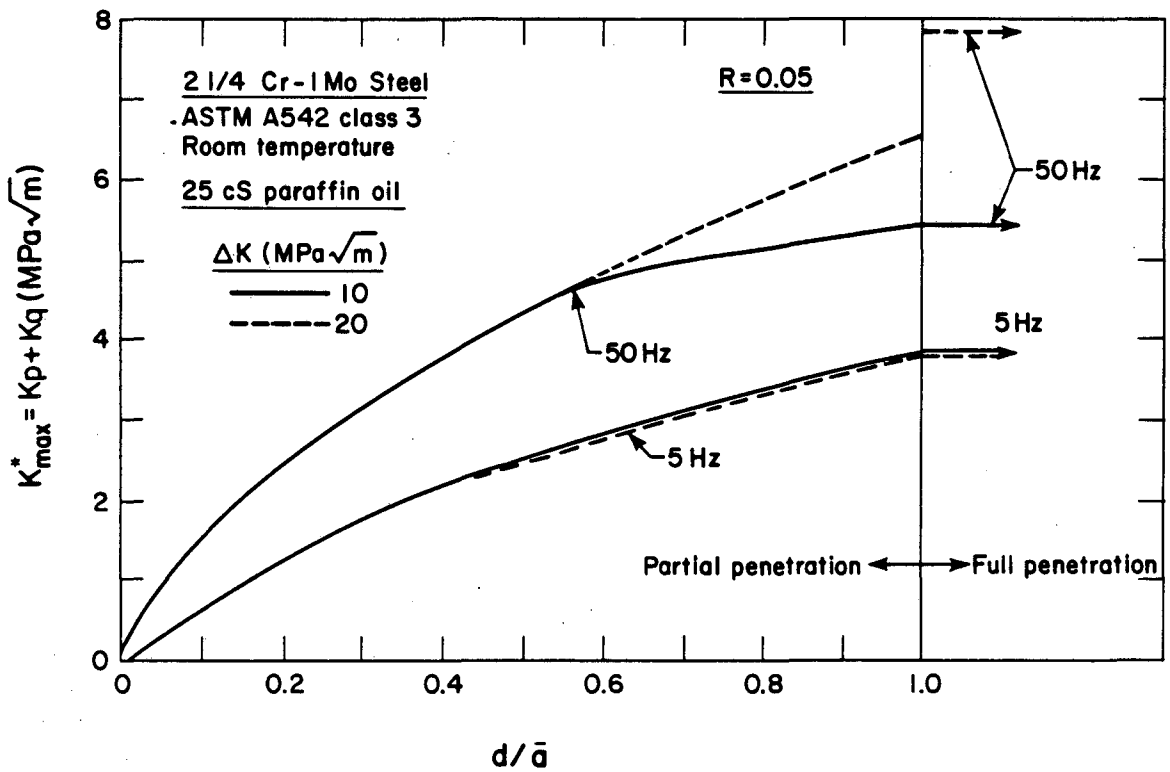

XBL 8311-3393

Fig. 14. Predicted effect of frequency on the value of $K^*_{max} = K_p + K_q$ as a function of normalized fluid penetration distance, $d/\bar{a}$, for ΔK = 10 and 20 MPa$\sqrt{m}$ (R = 0.05) in 25 cS paraffin oil. Predictions for 20 mm crack at 5 and 50 Hz from full penetration model ($d/\bar{a}$ = 1) in Eq. (15) and partial penetration model ($d/\bar{a}$ < 1) in Eq. (16).

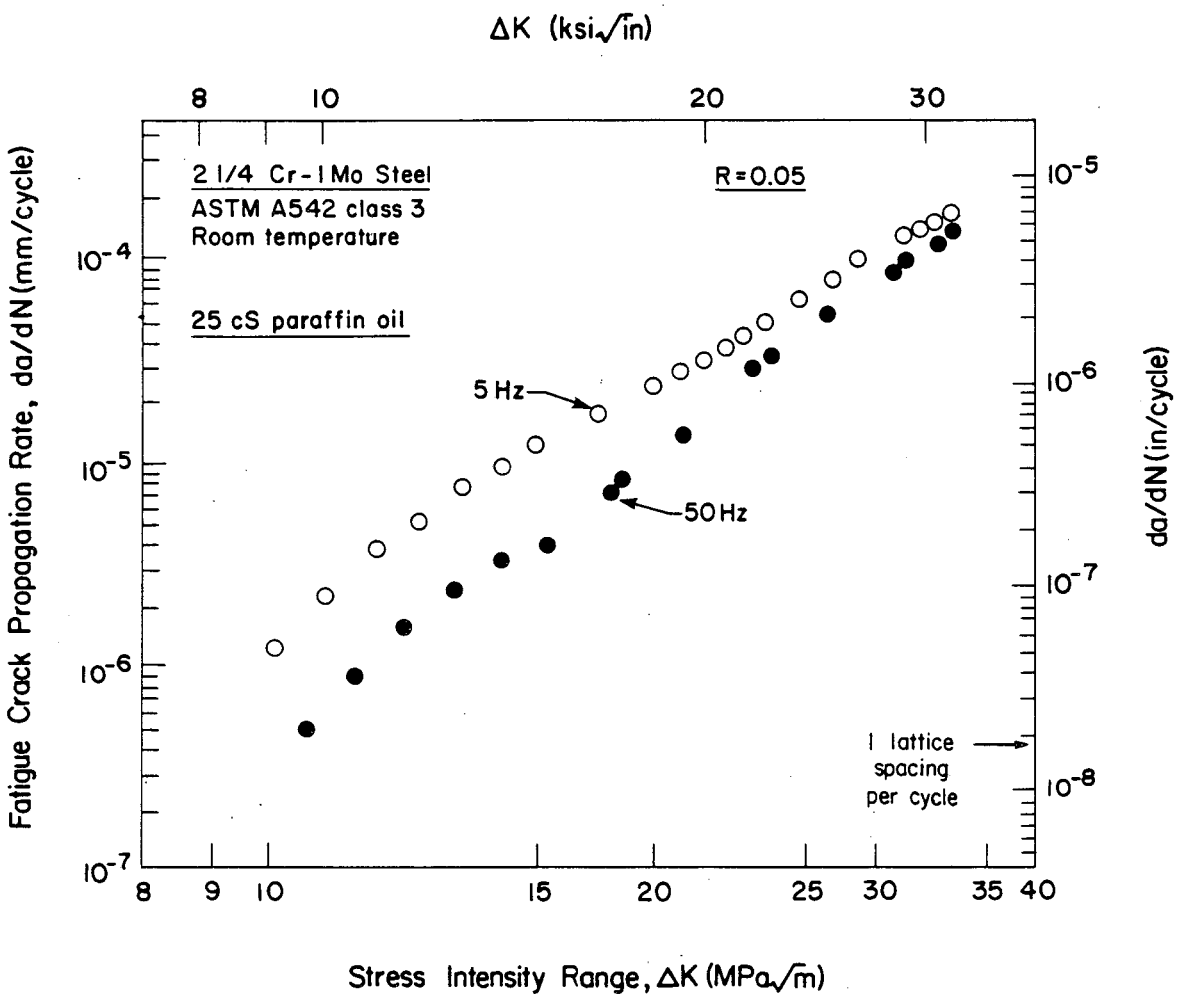

Fig. 15. Experimentally measured variation in fatigue crack propagation rates (da/dN) with hominal stress intensity range (ΔK) in bainitic 2¼Cr-1Mo steel tested in 25 cS paraffin oil at 5 and 50 Hz (R = 0.05).

This report was done with support from the Department of Energy. Any conclusions or opinions expressed in this report represent solely those of the author(s) and not necessarily those of The Regents of the University of California, the Lawrence Berkeley Laboratory or the Department of Energy.

Reference to a company or product name does not imply approval or recommendation of the product by the University of California or the U.S. Department of Energy to the exclusion of others that may be suitable.

TECHNICAL INFORMATION DEPARTMENT
LAWRENCE BERKELEY LABORATORY
UNIVERSITY OF CALIFORNIA
BERKELEY, CALIFORNIA 94720